

RESEARCH

Open Access



Characteristics of intestinal bacteriophages and their relationship with Bacteria and serum metabolites during quail sexual maturity transition

Xinwei Xiong^{1*†}, Jishang Gong^{1†}, Tian Lu¹, Liuying Yuan¹, Yuehang Lan¹ and Xutang Tu^{1*}

Abstract

Background Bacteriophages are prokaryotic viruses that rank among the most abundant microbes in the gut but remain among the least understood, especially in quails. In this study, we surveyed the gut bacteriophage communities in 22 quails at different ages (days 20 and 70) using shotgun metagenomic sequencing. We then systematically evaluated the relationships with gut bacteria and host serum metabolites.

Results We discovered that Myoviridae and Siphoviridae were the dominant bacteriophage families in quails. Through a random forest and LEfSe analysis, we identified 23 differential bacteriophages with overlapping presence. Of these, 21 bacteriophages (e.g., *Enterococcus phage IME-EFm5* and *Enterococcus phage IME-EFm1*) showed higher abundances in the day 20 group, while two bacteriophages (*Bacillus phage Silence* and *Bacillus virus WPh*) were enriched in the day 70 group. These key bacteriophages can serve as biomarkers for quail sexual maturity. Additionally, the differential bacteriophages significantly correlated with specific bacterial species and shifts in the functional capacities of the gut microbiome. For example, *Enterococcus* phages (e.g., *Enterococcus phage EFP01*, *Enterococcus phage IME-EFm5*, and *Enterococcus phage IME-EFm1*) were significantly ($P < 0.001$, FDR) and positively correlated with *Enterococcus faecalis*. However, the relationships between the host serum metabolites and either bacteriophages or bacterial species varied. None of the bacteriophages significantly ($P > 0.05$, FDR) correlated with nicotinamide riboside and triacetate lactone. In contrast, some differential bacterial species (e.g., *Christensenella massiliensis* and *Bacteroides neonati*) significantly ($P < 0.05$, FDR) correlated with nicotinamide riboside and triacetate lactone. Furthermore, characteristic successional alterations in gut bacteriophages, bacteria, and host serum metabolites across different ages highlighted a sexual maturity transition coexpression network.

[†]Xinwei Xiong and Jishang Gong contributed equally to this work.

*Correspondence:

Xinwei Xiong
XinweiXiong@hotmail.com
Xutang Tu
tuxutang@ncnu.edu.cn

Full list of author information is available at the end of the article



© The Author(s) 2024. **Open Access** This article is licensed under a Creative Commons Attribution 4.0 International License, which permits use, sharing, adaptation, distribution and reproduction in any medium or format, as long as you give appropriate credit to the original author(s) and the source, provide a link to the Creative Commons licence, and indicate if changes were made. The images or other third party material in this article are included in the article's Creative Commons licence, unless indicated otherwise in a credit line to the material. If material is not included in the article's Creative Commons licence and your intended use is not permitted by statutory regulation or exceeds the permitted use, you will need to obtain permission directly from the copyright holder. To view a copy of this licence, visit <http://creativecommons.org/licenses/by/4.0/>. The Creative Commons Public Domain Dedication waiver (<http://creativecommons.org/publicdomain/zero/1.0/>) applies to the data made available in this article, unless otherwise stated in a credit line to the data.

Conclusion This study improves our understanding of the gut bacteriophage characteristics in quails and offers profound insights into the interactions among gut bacteriophages, bacteria, and host serum metabolites during the quail's sexual maturity transition.

Keywords Quail, Gut microbiome, Bacteriophages, Metagenomic sequencing, Sexual maturity

Background

Emerging data suggest that viruses are integral members of the host microbiome, populating surfaces such as the gut, mouth, and skin [1–3]. The majority of these viruses that target bacteria are bacteriophages, often exhibiting species-level specificity [4]. Bacteriophages harbor numerous genetic functions, including platelet binding, complement and immunoglobulin degradation, and other gene functions, potentially offering significant advantages to their bacterial hosts [2, 5]. Moreover, the metagenomic composition of bacteriophages has been linked with diseases, such as malnutrition and inflammatory bowel disease [6, 7]. However, the actual behavior of bacteriophages in the gut, particularly in quails, remains undiscovered.

Bacteriophages are the most prolific biological entities on earth and significantly influence microbial communities [8, 9]. Their communities also react to disturbances, albeit differently than one might anticipate based on the responses of their bacterial hosts [10]. Bacteriophages can destroy host cells, alter host phenotypes via lysogenic conversion, and change bacterial communities through infection [11]. By influencing the stability of the intestinal microbiota, bacteriophages can mold the immunological and metabolic functions of the intestine [12]. Additionally, the bacteria-phage interactions and host-microbial relationships during the weaning transition affect host metabolism, resulting in advantageous host adaptations across the three weaning phases [4]. These studies indicate that phages play a pivotal role in shaping the gut bacterial community structure, and bacteria-phage interactions are crucial to bacterial physiology and metabolism.

Quails are significant poultry breeds and serve as essential sources of eggs and meat for human consumption. To date, few studies have concentrated on the alterations in the gut microbiome during quail sexual maturity. Our previous research identified five species that were abundant in the day 20 group (e.g., *Enterococcus faecalis*) and 12 species that were prevalent in the day 70 group (e.g., *Bacteroides neonati* and *Christensenella massiliensis*) as key bacterial markers for quail sexual maturity [13]. However, the quail bacteriophage interactions, bacteria-phage dynamics, and bacteriophage-serum metabolites interactions during sexual maturity transition remains unreported. In the present study, we gathered 22 fecal samples from quails at days 20 and 70 during sexual maturity transition phases and performed

shotgun metagenomic sequencing to exhaustively detail gut bacteriophage composition throughout this transition. Moreover, we also devised a co-occurrence network based on the relative abundances of different gut bacteriophages, bacterial species, and host serum metabolites during sexual maturity transition, aiming to further elucidate the intricacies of bacteria-phage interactions and their influence on host metabolism.

Results

Taxonomic characterization of quail Gut bacteriophage during sexual maturity transition

To probe the gut bacteriophage compositions of quails, we performed shotgun metagenomic sequencing on 22 fecal samples. The phylogenetic composition of the fecal bacteria was ascertained by performing a BLAST search against the National Center for Biotechnology Information (NCBI) non-redundant (NR) database. Within the 22 samples, a collective 15 families and 94 genera were identified. Myoviridae (spanning 11.15–89.26%) and Siphoviridae (spanning 4.19–60.10%) emerged as the two most predominant bacteriophage families in the quail gut microbiome (Fig. 1). At the genus level, the most prevalent genera in quails were *Cp220virus* and *Aviadenovirus*, boasting average abundances across samples of 11.73% and 9.33%, respectively, followed by *N4virus* and *Sfi21dt-Ivirus*. At the species level, a sum of 515 bacteriophage species were detected in the 22 samples. Among these, 22 species were discerned in over 90% of the analyzed samples, thus being categorized as core bacteriophages. *Phage DP-2017a* was the most abundant bacteriophage in the inspected samples, followed by *Enterococcus phage EFP01* and *Enterococcus phage IME-EFm5* (Fig. 2).

Bacteriophage differences during quail sexual maturity transition

To discern bacteriophage species associated with sexual maturity, we examined the differences in bacteriophage composition of the quail gut microbiome between the day 70 and day 20 cohorts. The Partial Least Squares-Discriminant analysis (PLS-DA) depicted a discernible shift in gut bacteriophages between day 70 and day 20 groups (Fig. 3A). As anticipated, linear discriminant analysis (LDA) effect size (LEfSe) analysis pinpointed 55 differential bacteriophages (Fig. 3B and Supplementary Table S1), including 49 species manifesting elevated abundance in the day 20 group and 6 species prominently enriched in the day 70 group. The day 20 group predominantly

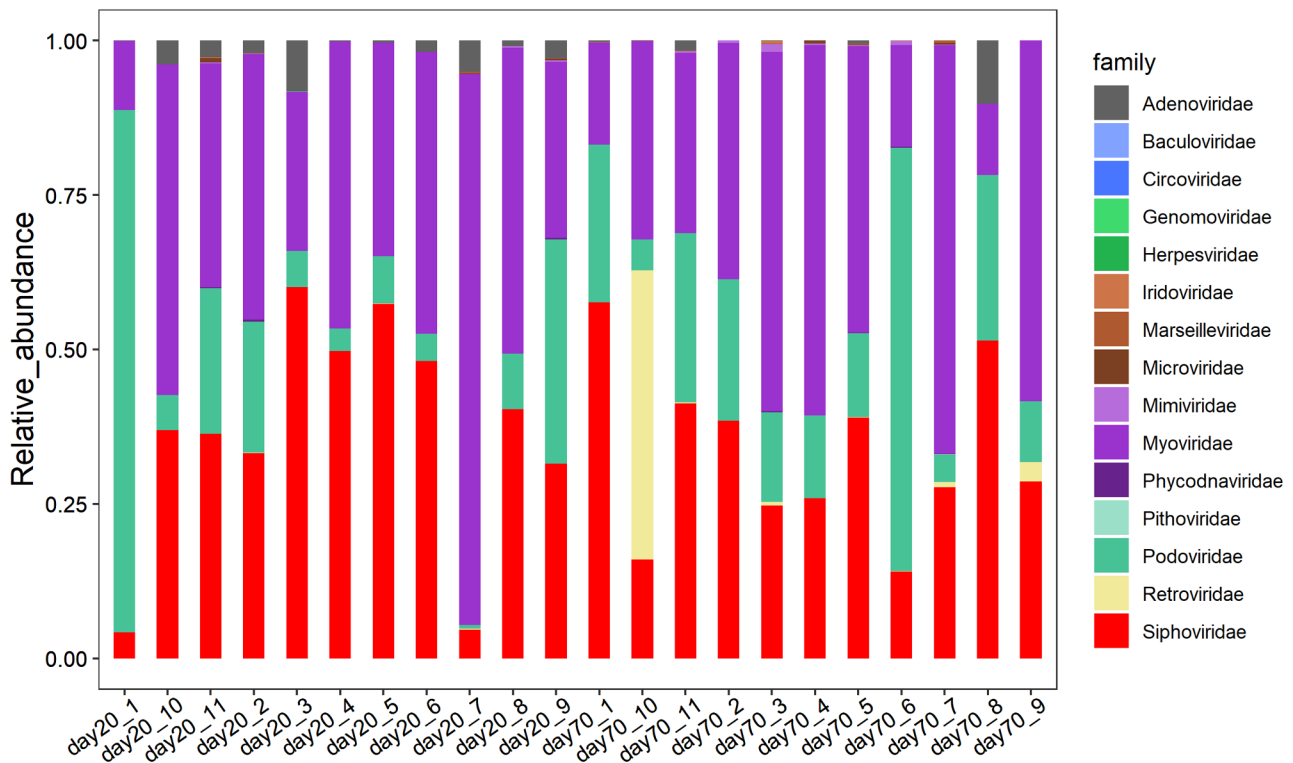


Fig. 1 Categories and relative abundance of gut bacteriophages at the family level based on shotgun metagenomic sequencing data from all tested samples

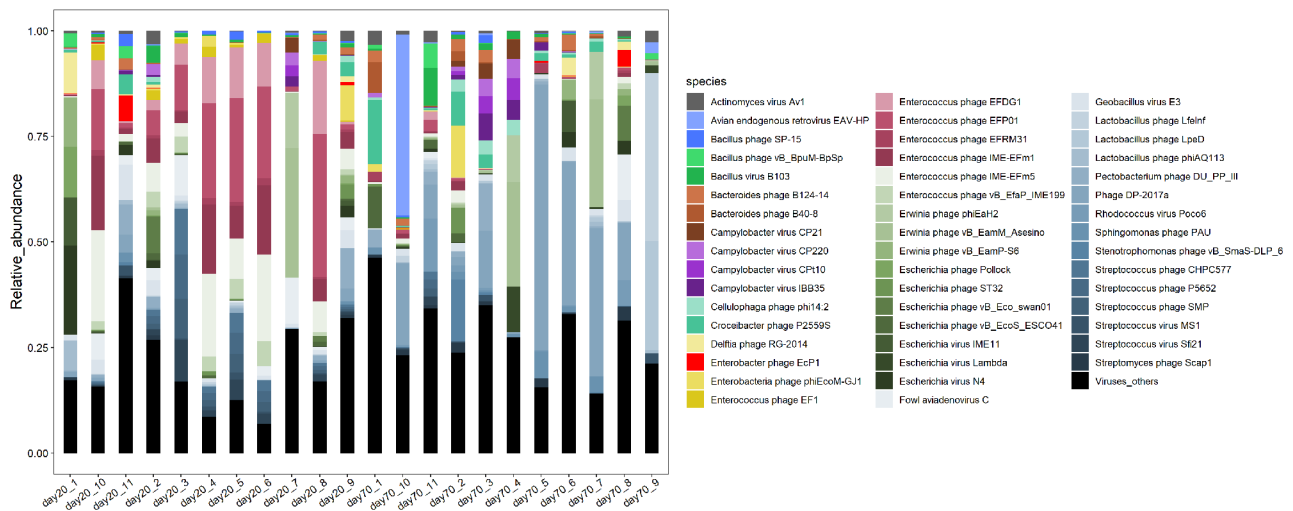


Fig. 2 Categories and relative abundance of gut bacteriophages at the species level based on shotgun metagenomic sequencing data from all tested samples

featured bacteriophages from the Siphoviridae family (21 species, e.g., *Enterococcus phage IME-EFm1*, *Enterococcus phage IME-EFm5*, and *Lactobacillus phage Lrm1*), Podoviridae (9 species, e.g., *Enterobacteria phage 285P*, *Enterobacteria phage EcoDS1*, and *Escherichia phage vB_EcoP_F*), and Myoviridae (9 species, e.g., *Bacillus virus Bcp1*, *Cronobacter virus PBES02*, and *Staphylococcus virus G1*). Conversely, the day 70 group saw enrichment

of species such as *Rhodococcus virus POCO6*, *Bacillus virus WPh*, *Croceibacter phage P2559Y*, *Bacillus phage Silence*, *Cronobacter phage S13*, and *Marinobacter phage PS6*. Moreover, a random forest analysis was deployed to pinpoint bacteriophage biomarkers that differentiated quail sexual maturity at the species level (Supplementary Fig. 1 and Supplementary Table S2). This unveiled that 28 bacteriophage species were significantly distinct between the

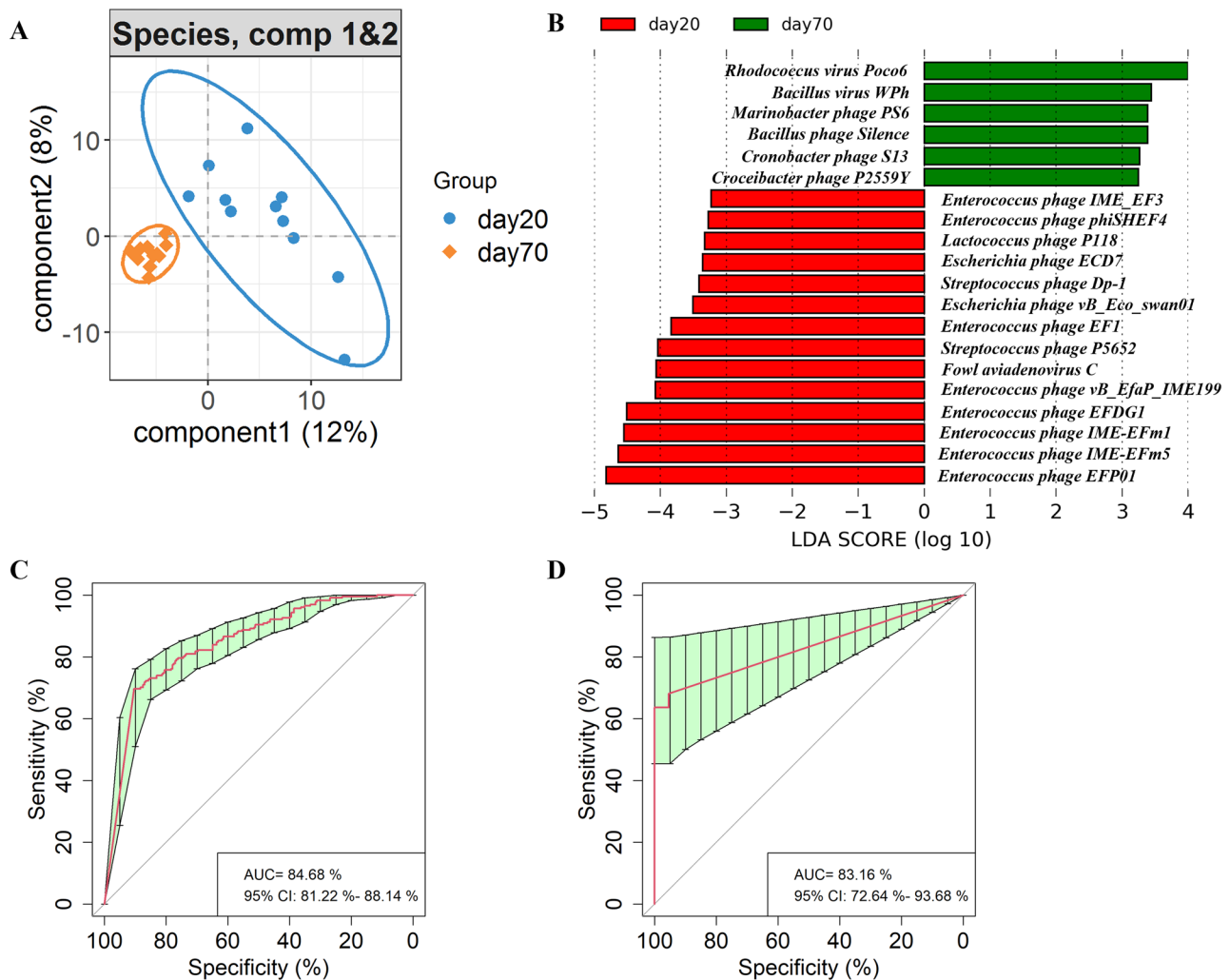


Fig. 3 Characteristics of gut bacteriophages between the day 70 and day 20 groups. **(A)** PLS-DA plot highlighting significantly different gut bacteriophage species between the day 70 and day 20 groups. **(B)** Differential gut bacteriophage species between the day 70 and day 20 groups. **(C)** and **(D)** Receiver operating curves (ROC) for the day 20 and day 70 groups, respectively

day 70 and day 20 cohorts, of which, 23 coincided with the LEfSe analysis (Supplementary Table S3). These overlapping bacteriophages enriched in either the day 20 or day 70 group served as potent markers differentiating the sexual maturity of quails boasting diagnostic accuracies of 84.68% and 83.16% respectively, as evidenced by the area under the curve (AUC) (Fig. 3C and D).

Bacteriophages associated with bacterial species during quail sexual maturity transition

In our previous study, 17 bacterial species, 21 KEGG pathways, and 25 CAZymes exhibited significant differences between the day 20 and day 70 groups. Specifically, five species were enriched on day 20 (e.g., *Enterococcus faecalis*) while 12 species were prevalent on day 70 (e.g., *Bacteroides neonati*, *Clostridium sp. CAG:217*, and *Christensenella massiliensis*). These bacterial species showed significant correlations with specific KEGG pathways

and CAZymes. To thoroughly evaluate the relationship between the bacteriophages and these differential bacterial species, we employed Spearman correlation analysis. Our findings showed that the bacterial species predominant in the day 20 group had significant ($P < 0.05$, FDR) and positive correlations with the bacteriophages predominant in the same day 20 group (Fig. 4). For instance, *Enterococcus faecalis* showed a significant ($P < 0.001$, FDR) and positive correlation with *Enterococcus* phages (e.g., *Enterococcus phage EFP01*, *Enterococcus phage IME-EFm5*, and *Enterococcus phage IME-EFm1*). *Streptococcus gallolyticus* and *Streptococcus equinus* significantly ($P < 0.001$, FDR) and positively correlated with *Streptococcus phage Dp-1* and *Streptococcus virus SPQS1*. For the day 70 group, *Bacillus virus WPh* had a significant ($P < 0.05$, FDR) and positive correlation with the bacterial species prevalent on day 70, and *Bacillus phage Silence* was significantly ($P < 0.05$, FDR) and positively correlated

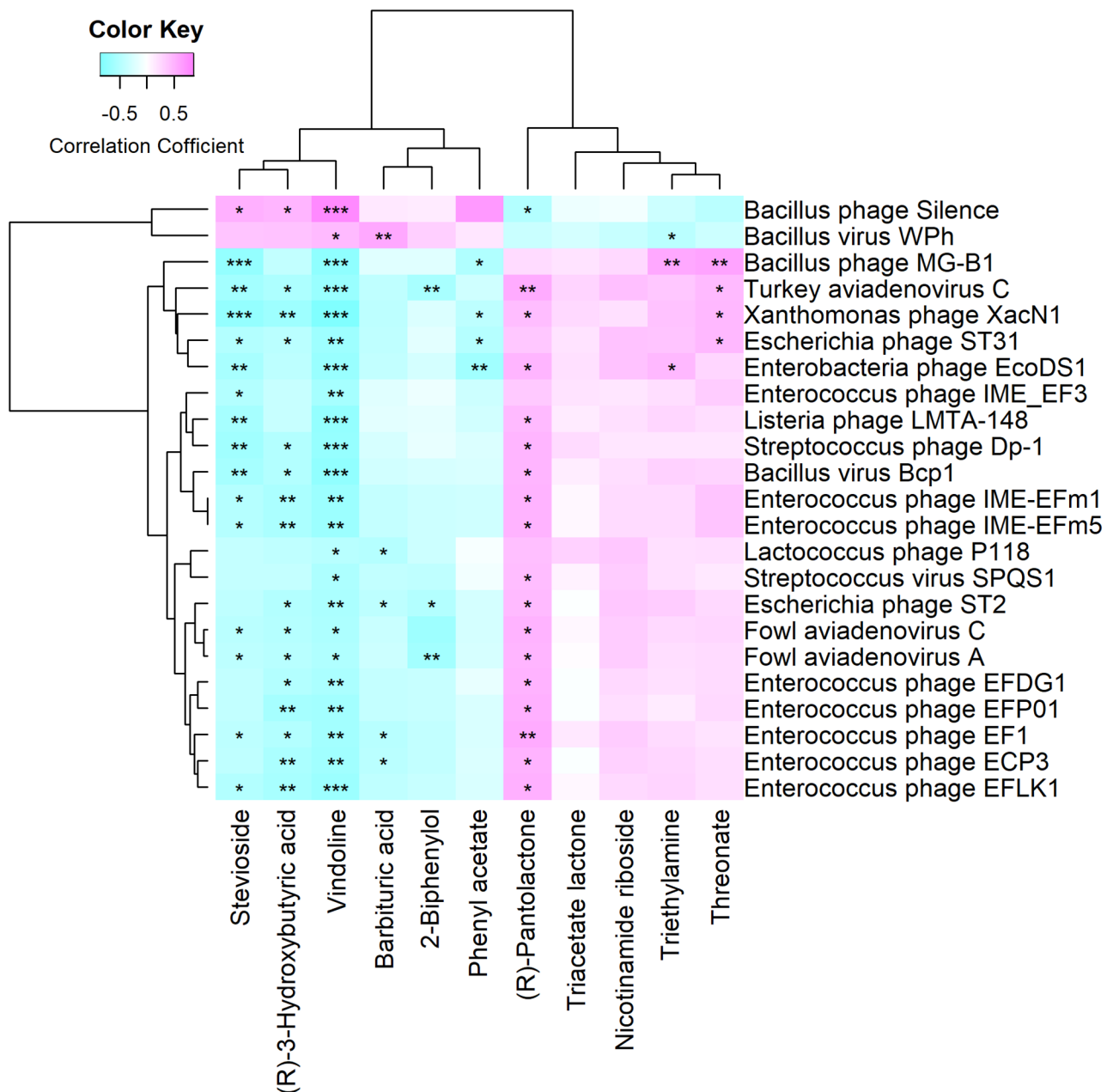


Fig. 5 Heat maps illustrating the relationships between differential gut bacteriophage species and differential serum metabolites. The X-axis denotes serum metabolites, while the Y-axis refers to bacteriophage species. Significance levels are denoted as: * $P < 0.05$, ** $P < 0.01$, and *** $P < 0.001$

significant ($P < 0.05$, FDR) negative correlation with vindoline and stevioside, both of which were enriched in the day 20 group. This mirrored the patterns observed with the bacterial species *Enterococcus faecalis*. Nonetheless, none of the bacteriophages exhibited a significant ($P < 0.05$, FDR) correlation with nicotinamide riboside and triacetate lactone (Fig. 5). As for differential bacterial species, triacetate lactone had a significant ($P < 0.05$, FDR) correlation with *Christensenella massiliensis* and *Clostridium sp. CAG:217*. Similarly, nicotinamide riboside showed significant ($P < 0.05$, FDR) correlations with

multiple bacterial species, including *Bacteroides neonati*, *Bacteroides luti*, *Bacteroides fingoldii*, *Bacteroidales bacterium WCE2004*, *Bacteroidales bacterium CF*, *Bacteroides sp. CAG:1060_57_27*, *Alistipes sp. CAG:831*, and *Megasphaera sp. An286*.

Co-occurrence analysis among the gut bacteriophages, bacteria, and serum metabolites

We delved further into the potential correlations among gut bacteriophages, host serum metabolites, and differential bacterial species by using co-occurrence network

analysis. The analysis revealed that the gut bacteriophages, host serum metabolites, and differential bacterial species predominantly formed six clusters, exhibiting robust and extensive co-occurrence relationships (Fig. 6). Gut bacteriophages predominant in the day 20 group were chiefly situated in clusters 5 and 6. In contrast, differential bacterial species more common in the day 70 group were predominantly found in cluster 1. Additionally, serum metabolites abundant in the day 20 group populated cluster 3, while cluster 4 comprised six host serum metabolites that were more prevalent in the day 70 group. Notably, *Bacillus virus WPh*, which was enriched in the day 70 group, displayed a positive and significant correlation with bacterial species (e.g., *Christensenella massiliensis*, *Clostridium sp. CAG:217*, and *Bacteroides neonati*) located in cluster 1. In contrast, *Streptococcus gallolyticus* and *Streptococcus equinus*, which were more abundant in the day 20 group, showed a positive and significant correlation with bacteriophages (e.g., *Streptococcus phage Dp-1* and *Streptococcus virus SPQ51*) found in cluster 6.

Discussion

Bacteriophages play multifaceted roles in microbial evolution and ecology [14]. Although the bacterial components of the microbiome have garnered considerable attention, the composition and physiological significance

of bacteriophages, especially in quails remain relatively unexplored. In this study, we systematically assessed the impact of host sexual maturity on the gut bacteriophage composition in quails aged between 20 and 70 days using metagenomic sequencing data. We also examined the relationships between bacteriophages, different bacterial species, functional capacities of the gut microbiome, and host serum metabolites. To the best of our knowledge, this study is the first to delve into the interplay among bacteriophages, bacterial species, and host serum metabolites.

In the current study, Myoviridae and Siphoviridae emerged as the two predominant bacteriophage families in quails. Phages within the Myoviridae and Siphoviridae families share an evolutionary lineage with other cellular biological entities that possess the shared function of penetrating bacterial envelopes [15]. Furthermore, Myoviridae employ double-layered contractile tails to infect bacteria [16] and are primarily shaped by vertical evolution as opposed to horizontal gene transfer [17, 18]. Our analysis, using LEfSe and random forest, identified 23 differential bacteriophages, of which eight were *Enterococcus* phages. Combinations of *Enterococcus* phages have demonstrated greater efficacy than single phages in thwarting the proliferation of antibiotic- and phage-resistant *Enterococcus* mutants in vitro [19, 20]. Notably, we observed that *Enterococcus* phages significantly

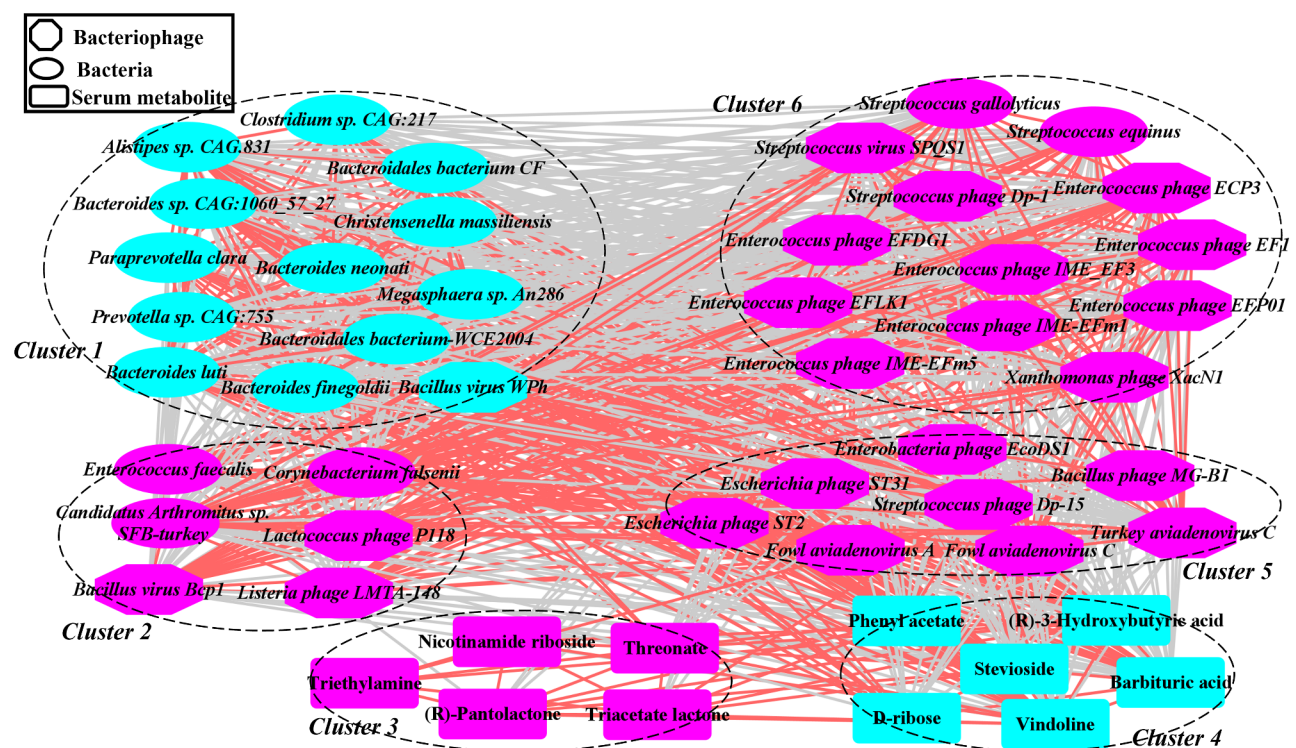


Fig. 6 A co-occurrence network built from gut bacteriophages, bacterial species, and host serum metabolites, highlighting differences in abundance between the day 70 and day 20 groups. The purple and blue dots represent the day 20 and day 70 groups, respectively. Edges between nodes depict Spearman's negative (light grey) or positive (light red) correlations

($P < 0.001$, FDR) and positively correlated with *Enterococcus faecalis*. Additionally, *Streptococcus gallolyticus* and *Streptococcus equinus* displayed significant positive correlations with *Streptococcus phage Dp-1* and *Streptococcus virus SPQS1*, respectively ($P < 0.001$, FDR). A previous study by Patterson and Burkholder revealed that several microbial species (e.g., *Enterococcus*, and *Streptococcus*) used as probiotics can diminish poultry mortality across various ages, and enhance growth rates and feed efficiency [21]. These findings suggest that bacteriophage interactions could be pivotal for quail adaptation during the sexual maturity transition.

Spearman correlation analysis revealed that all differential bacteriophages significantly correlated with vindoline ($P < 0.05$, FDR). Vindoline, a monomeric Vinca alkaloid, is a natural monomer known for its anti-inflammatory properties [22, 23]. Specifically, the *Enterococcus phage IME_EF3* shared a correlation with *Enterococcus faecalis* in the day 20 cohort. This phage possesses an isometric head and a lengthy non-contractile tail, with a 41 kb linear double-stranded DNA genome encoding 69 putative proteins, 32 of which have annotated function [24]. However, *Enterococcus phage IME_EF3* is not apt for phage therapy against *Enterococcus faecalis* unless one could excise the metallo-beta-lactamase gene; however, its lysin might prove beneficial in treating *Enterococcus faecalis* infections [24]. Contrarily, unlike the differential bacterial species, none of the bacteriophages displayed a significant correlation with nicotinamide riboside or triacetate lactone ($P > 0.05$, FDR). Nicotinamide ribose is known to ameliorate metabolic dysfunctions and lower various inflammatory cytokine levels [25]. These observations imply that bacteriophage-host and bacteria-host interactions may differ, but both are crucial for quail adaptation during their sexual maturity transition.

Conclusion

In summary, we observed significant alterations in gut bacteriophage composition during the sexual maturity processes in quails. A total of 23 differential bacteriophages were identified using LEfSe and random forest analysis, serving as the key biomarkers for quail sexual maturity. These differential bacteriophages notably correlate with specific bacterial species. The differential bacteriophages and bacterial species share correlations with KEGG pathways and CAZymes, but not with serum metabolites. This study provides valuable insights into the interactions among gut bacteriophages, bacteria, and serum metabolites in quails. Nevertheless, the causality and underlying mechanisms remain undefined, which will be the focus of future research.

Methods

Sample collection and microbial DNA extraction

In this study, we incorporated a total of 22 quail samples from Jiangxi Hengyan Poultry Co. Ltd. (Fengcheng, Jiangxi, China), including 10 Japanese quails (7 females and 3 males) and 12 Hengyan white feather quails (6 females and 6 males). The quails were given *ad libitum* access to clean water and a commercial formula (Supplementary Table S4), and were maintained under uniform management conditions and environment. Based on previous research [26], we designated quails aged 20 days old as representing the pre-sexual maturity stage and those aged 70 days old as the post-sexual maturity stage, including 11 quails aged 20 days and 11 quails aged 70 days. Fresh fecal samples were obtained using a rectal kneading method from each quail on days 20 and 70. Throughout our study, all quails remained in a healthy condition, with no evident illnesses or medical treatments from birth to the conclusion of our research. The gathered fecal samples were promptly frozen in liquid nitrogen for transit, and subsequently stored at $-80\text{ }^{\circ}\text{C}$ until further analysis. Blood samples were simultaneously collected from each quail.

Microbial DNA from the 22 quail samples was extracted utilizing the QIAamp Fast DNA Stool Mini Kit (Qiagen, Germany), according to the manufacturer's instructions. The DNA concentration and quality was assessed by a Nanodrop-2000 spectrophotometer (Thermo Fisher Scientific, MA, US) and 0.8% (w/v) agarose gel electrophoresis, respectively. All extracted fecal microbial DNA samples were preserved at $-20\text{ }^{\circ}\text{C}$ for future use.

Metagenomic sequencing and analysis

Metagenomic sequencing of all 22 microbial DNA samples was carried out on the Novaseq-PE150 platform. Following the manufacturer's instructions, we generated a paired-end sequencing library with an insert size of 350 bp using the NEB Next[®] Ultra[™] DNA Library Prep Kit (NEB, USA). Index codes were appended to attribute the sequences to their corresponding samples. The Agilent 2100 Bioanalyzer facilitated the evaluation of the library's size distribution. Subsequently, the libraries were sequenced and quantified on Novaseq 6000 platform (Illumina, USA) and real-time PCR.

To curate the raw sequencing data, we eliminated adapters and purged low-quality reads. The Bowtie2.2.4 software [27] was then employed to remove host contamination by referencing against the quail genome (INSDC: LSZS01000000). Clean data assembly was achieved using the SOAPdenovo software (v.2.21) [28, 29]. MetaGeneMark (V2.10) [29, 30] was used to predict open reading frames (ORF) with the contigs longer than 500 bp. The gene catalog (Unigenes) was derived by eliminating

redundant genes from all predicted ORFs via the Cluster Database at High Identity with Tolerance (CD-HIT) software [31]. These Unigenes were then aligned to bacteriophage sequences extracted from the NCBI NR database using the DIAMOND software [32]. Results were refined to include only those with an e value \leq the smallest e value $\times 10$ [33], using the LCA algorithm incorporated into the MEGAN [34] classification software.

Metabolomic profile determination of quail serum samples

As described in our previous study [13], the untargeted metabolomics was used to determine the metabolomic profiles of all 22 quail serum samples. A mixture of 400 μ L precooled methanol and 100 μ L quail serum was vortexed. LC-MS/MS analysis was then performed using a Vanquish UHPLC system (Thermo Fisher) coupled to an Orbitrap Q Exactive series mass spectrometer (Thermo Fisher Scientific). Raw data files generated by UHPLC-MS/MS were processed using Compound Finder 3.0 (CD3.0, Thermo Fisher), to determine lignent, peak pickup, and quantification of each metabolite. R (R version R-3.4.3), Python (Python 2.7.6 version), and CentOS (CentOS release 6.6) software was used to perform subsequent statistical analysis.

Statistical analysis

Linear discriminant analysis (LDA) and effect size (LEfSe) analysis were performed under the criterion of $\alpha=0.01$, and an LDA score threshold of at least 2.50 [35]. Random forest analysis incorporating adjusted settings (ntree=1000) was employed to pinpoint gut bacteriophage species pivotal for distinguishing sexual maturity stages in quails [36]. The associations between gut bacteriophage species and differential bacterial species, differential KEGG pathways, differential CAZymes, and host serum metabolites were gauged via Spearman correlation analysis. Multiple tests were adjusted using Story's false discovery rate (FDR). Partial least squares-discriminant analysis (PLS-DA) was undertaken to contrast gut bacteriophage species between the day 70 and day 20 cohorts [37]. Co-abundance (indicated as positive) and co-exclusion (represented as negative) relationships among differential gut bacteriophages, bacterial species, and host serum metabolites were discerned through Sparse correlations for compositional data (SparCC) [35], predicated on their relative abundance metrics. For a visual representation of the intricate relationships, network analysis was orchestrated and visualized in Cytoscape (v 3.6.1) [38].

Abbreviations

AUC	area under the curve
bp	base-pairs
CAZy	Carbohydrate-Active enZYmes database
CD-HIT	Cluster Database at High Identity with Tolerance

FDR	false discovery rate
NCBI	National Center for Biotechnology Information
NR	non-redundant
ORF	open reading frames
PLS-DA	Partial least squares-discriminant analysis
KEGG	Kyoto Encyclopedia of Genes and Genomes
SparCC	Sparse Correlations for Compositional
LDA	linear discriminant analysis
LEfSe	linear discriminant analysis effect size

Supplementary Information

The online version contains supplementary material available at <https://doi.org/10.1186/s12917-024-03945-9>.

Supplementary Material 1: Figure S1. Random Forest analysis to determine our ability to discriminate samples from different sexual maturity periods based on gut bacteriophage species

Author contributions

XX. conceived and designed the experiments, analyzed data, wrote and revised the manuscript. J.G. performed the experiments and revised the manuscript. T.L. analyzed the data. L.Y. and Y.L. performed the experiments. X.T. conceived and designed the experiments, and revised the manuscript. All authors read and approved the final manuscript.

Funding

This work was supported by the ShuangQian planning Projects of Jiangxi Province and Jiangxi Joint Key Project of Quail Improvement (2022JXCQZY02).

Data availability

The metagenomic sequence datasets provided in this study can be found in the online repository. The name and login number of the repository are as follows: NCBI SRA Bioproject, login number: PRJNA861719.

Declarations

Ethics approval and consent to participate

The study was carried out in compliance with the ARRIVE guidelines. All animal work was conducted according to the guidelines for the care and use of experimental animals established by the State Council of the People's Republic of China (Decree No. 2, 1988). This study was also approved by the Animal Care and Use Committee (ACUC) of Nanchang Normal University (No. NCNU2020-008). We got the permission from Jiangxi Hengyan Poultry Co. Ltd. to collect the samples of quails.

Consent for publication

Not applicable.

Competing interests

All authors declare no conflicts of interest, financial or otherwise.

Author details

¹Jiangxi Provincial Key Laboratory of Poultry Genetic Improvement, Nanchang Normal University, Nanchang, Jiangxi 330032, China

Received: 16 October 2023 / Accepted: 20 February 2024

Published online: 08 March 2024

References

- Hannigan GD, Meisel JS, Tyldsley AS, Zheng Q, Hodkinson BP, SanMiguel AJ, et al. The human skin double-stranded DNA virome: topographical and temporal diversity, genetic enrichment, and dynamic associations with the host microbiome. *mBio*. 2015;6:e01578–01515.
- Pride DT, Salzman J, Haynes M, Rohwer F, Davis-Long C, White RA 3, et al. Evidence of a robust resident bacteriophage population revealed through analysis of the human salivary virome. *ISME J*. 2012;6:915–26.

3. Minot S, Sinha R, Chen J, Li H, Keilbaugh SA, Wu GD, et al. The human gut virome: inter-individual variation and dynamic response to diet. *Genome Res.* 2011;21:1616–25.
4. Xiong X, Liu X, Wang Z, Xu Q, Xu J, Rao Y. Identifying biomarkers of the gut bacteria, bacteriophages and serum metabolites associated with three weaning periods in piglets. *BMC Vet Res.* 2022;18:104.
5. Willner D, Furlan M, Schmieder R, Grasis JA, Pride DT, Relman DA, et al. Metagenomic detection of phage-encoded platelet-binding factors in the human oral cavity. *Proc Natl Acad Sci U S A.* 2011;108(Suppl 1):4547–53.
6. Norman JM, Handley SA, Baldridge MT, Droit L, Liu CY, Keller BC, et al. Disease-specific alterations in the enteric virome in inflammatory bowel disease. *Cell.* 2015;160:447–60.
7. Reyes A, Blanton LV, Cao S, Zhao G, Manary M, Trehan I, et al. Gut DNA viromes of Malawian twins discordant for severe acute malnutrition. *Proc Natl Acad Sci U S A.* 2015;112:11941–6.
8. Weinbauer MG. Ecology of prokaryotic viruses. *FEMS Microbiol Rev.* 2004;28:127–81.
9. Paez-Espino D, Eloe-Fadrosh EA, Pavlopoulos GA, Thomas AD, Huntemann M, Mikhailova N, et al. Uncovering Earth's virome. *Nature.* 2016;536:425–30.
10. Ly M, Jones MB, Abeles SR, Santiago-Rodriguez TM, Gao J, Chan IC, et al. Transmission of viruses via our microbiomes. *Microbiome.* 2016;4:64.
11. Kim MS, Bae JW. Lysogeny is prevalent and widely distributed in the murine gut microbiota. *ISME J.* 2018;12:1127–41.
12. Zeng Y, Wang Z, Zou T, Chen J, Li G, Zheng L, et al. Bacteriophage as an alternative to antibiotics promotes growth performance by regulating intestinal inflammation, intestinal barrier function and gut microbiota in weaned piglets. *Front Vet Sci.* 2021;8:623899.
13. Xiong X, Xu J, Yan X, Wu S, Ma J, Wang Z, et al. Gut microbiome and serum metabolome analyses identify biomarkers associated with sexual maturity in quails. *Poult Sci.* 2023;102:102762.
14. Zhao X, Skurnik M. Bacteriophages of *Yersinia pestis*. *Adv Exp Med Biol.* 2016;918:361–75.
15. Scholl D. Phage Tail-like Bacteriocins. *Annu Rev Virol.* 2017;4:453–67.
16. Novacek J, Saborova M, Benesik M, Pantucek R, Doskar J, Plevka P. Structure and genome release of Twort-like Myoviridae phage with a double-layered baseplate. *Proc Natl Acad Sci U S A.* 2016;113:9351–6.
17. Rohwer F, Edwards R. The phage proteomic tree: a genome-based taxonomy for phage. *J Bacteriol.* 2002;184:4529–35.
18. Lavigne R, Darius P, Summer EJ, Seto D, Mahadevan P, Nilsson AS, et al. Classification of Myoviridae bacteriophages using protein sequence similarity. *BMC Microbiol.* 2009;9:224.
19. Khalifa L, Gelman D, Shlezinger M, Copenhagen-Glazer S, Beyth N, et al. Defeating antibiotic- and phage-resistant *Enterococcus faecalis* using a phage cocktail in Vitro and in a clot model. *Front Microbiol.* 2018;9:326.
20. Wandro S, Ghatbale P, Attai H, Hendrickson C, Samillano C, Suh J, et al. Phage Cocktails Constrain Growth *Enterococcus mSystems.* 2022;7:e0001922.
21. Patterson JA, Burkholder KM. Application of prebiotics and probiotics in poultry production. *Poult Sci.* 2003;82:627–31.
22. Mayer S, Nagy N, Keglevich P, Szigetvari A, Dekany M, Szantay Junior C, et al. Synthesis of Novel Vindoline-Chrysin hybrids. *Chem Biodivers.* 2022;19:e202100725.
23. Zhang X, Zuo L, Geng Z, Song X, Li J, Ge S, et al. Vindoline ameliorates intestinal barrier damage in Crohn's disease mice through MAPK signaling pathway. *FASEB J.* 2022;36:e22589.
24. Li X, Ding P, Han C, Fan H, Wang Y, Mi Z, et al. Genome analysis of *Enterococcus faecalis* bacteriophage IME-EF3 harboring a putative metallo-beta-lactamase gene. *Virus Genes.* 2014;49:145–51.
25. Elhassan YS, Kluckova K, Fletcher RS, Schmidt MS, Garten A, Doig CL, et al. Nicotinamide Riboside augments the aged human skeletal muscle NAD(+) metabolome and induces transcriptomic and anti-inflammatory signatures. *Cell Rep.* 2019;28:1717–1728e1716.
26. Madekurozwa MC. Immunolocalization of intermediate filaments and laminin in the oviduct of the immature and mature Japanese quail (*Coturnix coturnix japonica*). *Anat Histol Embryol.* 2014;43:210–20.
27. Zhao W, Wang Y, Liu S, Huang J, Zhai Z, He C, et al. The dynamic distribution of porcine microbiota across different ages and gastrointestinal tract segments. *PLoS ONE.* 2015;10:e0117441.
28. Konopka A. What is microbial community ecology? *ISME J.* 2009;3:1223–30.
29. Mach N, Berri M, Estelle J, Levenez F, Lemonnier G, Denis C, et al. Early-life establishment of the swine gut microbiome and impact on host phenotypes. *Environ Microbiol Rep.* 2015;7:554–69.
30. Vo N, Tsai TC, Maxwell C, Carbonero F. Early exposure to agricultural soil accelerates the maturation of the early-life pig gut microbiota. *Anaerobe.* 2017;45:31–9.
31. Hamer HM, Jonkers D, Venema K, Vanhoutvin S, Troost FJ, Brummer RJ. Review article: the role of butyrate on colonic function. *Aliment Pharmacol Ther.* 2008;27:104–19.
32. De Filippis F, Pasolli E, Tett A, Tarallo S, Naccarati A, De Angelis M, et al. Distinct genetic and functional traits of human intestinal *Prevotella copri* strains are Associated with different habitual diets. *Cell Host Microbe.* 2019;25:444–453e443.
33. Pedersen HK, Gudmundsdottir V, Nielsen HB, Hyotylainen T, Nielsen T, Jensen BA, et al. Human gut microbes impact host serum metabolome and insulin sensitivity. *Nature.* 2016;535:376–81.
34. Flint HJ, Bayer EA, Rincon MT, Lamed R, White BA. Polysaccharide utilization by gut bacteria: potential for new insights from genomic analysis. *Nat Rev Microbiol.* 2008;6:121–31.
35. Segata N, Izard J, Waldron L, Gevers D, Miropolsky L, Garrett WS, et al. Metagenomic biomarker discovery and explanation. *Genome Biol.* 2011;12:R60.
36. He M, Gao J, Wu J, Zhou Y, Fu H, Ke S, et al. Host gender and androgen levels regulate gut bacterial taxa in pigs leading to sex-biased serum metabolite profiles. *Front Microbiol.* 2019;10:1359.
37. Kelly RS, McGeachie MJ, Lee-Sarwar KA, Kachroo P, Chu SH, Virkud YV et al. Partial Least Squares Discriminant Analysis and bayesian networks for Metabolomic Prediction of Childhood Asthma. *Metabolites.* 2018; 8.
38. Zhang Q, Wu Y, Wang J, Wu G, Long W, Xue Z, et al. Accelerated dysbiosis of gut microbiota during aggravation of DSS-induced colitis by a butyrate-producing bacterium. *Sci Rep.* 2016;6:27572.

Publisher's Note

Springer Nature remains neutral with regard to jurisdictional claims in published maps and institutional affiliations.